Vol. 569: 55–75, 2017
https://doi.org/10.3354/meps12102

MARINE ECOLOGY PROGRESS SERIES
Mar Ecol Prog Ser

Published April 7

Phytoplankton biomass in a subtropical estuary: drivers, blooms, and ecological functions assessed over space and time using structural equation modeling

C. Edward Proffitt*

Department of Life Sciences, Texas A&M University – Corpus Christi, Corpus Christi, TX 78412, USA

ABSTRACT: The Indian River Lagoon (IRL Florida, USA) estuary may be in transition from a benthic productivity state to a phytoplankton-based state because of nutrient inputs, phytoplankton blooms, and light penetration. Variation over both spatial and temporal dimensions reflects a complex ecological topology in the IRL. Understanding features such as phytoplankton blooms and subsequent effects on light penetration, dissolved oxygen, and benthic systems is challenging because of the underlying complexity. Analysis by structural equation modeling can test multivariate hypotheses involving the web of pathways linking biotic and environmental variables. A complex structural equation model composed of linkages among chlorophyll, nutrients, salinity, light penetration, dissolved oxygen (DO), etc. explained phytoplankton biomass (chl *a*, $R^2 = 0.46$) and relative abundance (chl *b* and *c*) and ecological functions (light penetration, $R^2 = 0.60$; DO, $R^2 = 0.42$) across the IRL and over the >20 yr of monitoring data. Results indicate that IRL experiences nitrogen and phosphorus co-limitation of phytoplankton, and that changes in plankton biomass influence ecological functions of DO and light penetration. Partitioning the IRL into regions improved the model fit to observations and showed that different regions of the IRL had different drivers for phytoplankton biomass. Comparing 3 yr groups of data for long and short water residence time regions showed that phytoplankton blooms in the 2010–2012 period (including the 'superbloom') were driven primarily by nitrogen and less by phosphorus and that this was associated in part by decomposing phytoplankton producing high concentrations of phosphorus during this period, leading to limitation by nitrogen.

KEY WORDS: Phytoplankton · Chlorophyll *a* · Structural equation modeling · Nutrient · Salinity · Temperature · Indian River Lagoon · Florida

INTRODUCTION

Many factors operating alone and in concert affect biotic communities. A suite of physio-chemical, biotic, and other factors establishes a complex ecological topology (see Thompson et al. 2001) in space and time. Adequate understanding of communities and ecosystems depends on analyzing the direct and indirect web of effects revolving around these factors (Grace 2006, Grace et al. 2010). Indeed, analyzing only direct effects can lead to spurious results. Harnik (2011) found that range distribution had a direct effect on bivalve extinction, but the only effect of abundance was through its indirect effects on range size. Ecological shifts, for example due to changes in climate, may vary because of differences in nutrient regimes, introduction of non-native species and shifts in the ranges of native species, cycles due to oscillations between El Niño, normal, and La Niña years, and seasonality.

Changes in nutrient regimes can produce shifts in primary productivity that result in a cascade of

*Corresponding author: ed.proffitt@tamucc.edu

effects through communities. In extreme cases, this can culminate in regime shifts to novel dominance suites. The Park Grass Experiment in England revealed that long-term (1859–present) fertilization treatments can reduce grassland plant biodiversity via increases in biomass, alter the composition of plant functional groups and food webs, and even change the trajectory of evolution (Silvertown et al. 2006). In estuaries, nutrient loading drives phytoplankton blooms that may lead to shifts from benthic to planktonic-dominated primary productivity (Kemp et al. 2005). For example, blooms of brown tide algae in Maryland (USA) coastal bays are linked to increases in nitrogen that directly affect estuarine biota (Glibert et al. 2007). Such changes from benthic to plankton dominance have profound effects on faunal populations that utilize the benthic system for habitat and food. If the novel dominance suite is maintained over a long time, then this may constitute a regime shift. Long-term effects of regime shifts in estuaries are not well understood, but may be as profound as those in the Park Grass analysis.

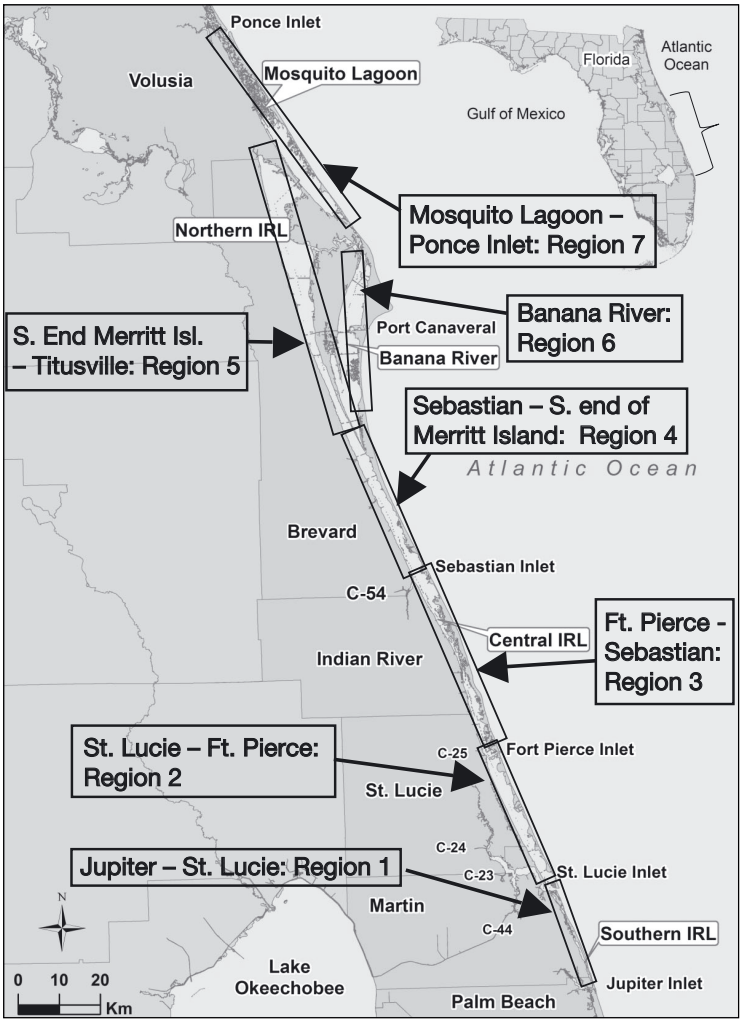

Fig. 1. Indian River Lagoon, Florida (USA), and the locations of the 7 study regions

The Indian River Lagoon (IRL) estuarine system is a long (≈250 km), narrow, and shallow series of subtropical estuaries on Florida's Atlantic coast (Fig. 1). The entire IRL system of estuaries covers some 89 000 ha, of which ≈80% is less than 1.8 m deep (Fletcher & Fletcher 1995). Much of the system is characterized by clear water most of the time, which allows extensive seagrass beds to develop and dominate the primary productivity of the subtidal regions (Thompson 1978, Short et al. 1993, Dawes et al. 1995). Intertidal habitats are dominated by mangroves in the south and mixed salt marsh–mangrove in the north.

Sigua et al. (2000) suggested that excess nutrients in the IRL may be causing a shift from a state dominated by benthic primary producers to one dominated by planktonic species. Most evidence for this comes from more northern regions of the IRL, where the proximity, number, and size of inlets results in a longer water residence time (Smith 1993, Smith pers. comm.). In recent years, these northern regions of the IRL have experienced increased nutrient loads and phytoplankton blooms (Phlips et al. 2011) that have been implicated in reduced light penetration which may have adversely affected seagrass and perhaps macroalgae abundance (Morris et al. 2015). In 2010 and 2011, the IRL region north of Sebastian Inlet experienced 2 major phytoplankton blooms, the second so massive that it is referred to as the 'superbloom' (SJRWMD 2012). Farther north, in the Mosquito Lagoon segment of the IRL, a 'brown tide' bloom occurred in 2012 (Gobler et al. 2013, Phlips et al. 2015). Because of considerable differences in tidal flushing and riverine inputs, both spatial and temporal variability of many variables (e.g. salinity, nutrients, chlorophylls, turbidity) seem likely to be considerable in this system. The relationships among phytoplankton and environmental variables were tested by analyzing data from the IRL estuarine system. If the IRL system is really undergoing a state change from dominance by benthic to planktonic primary production, then implications for consumer communities and resident endangered species could be profound.

Historically, the response to nutrient changes was viewed through the lens of Liebig's Law of Minimum (Danger et al. 2008), which posits that the single nutrient in the lowest supply controls primary production. More recent evidence suggests that primary production can be co-limited by multiple nutrients, and that combinations of nutrients can have a synergistic effect (Harpole et al. 2011). Mechanisms for co-limitation include different species in the assemblage or various metabolic pathways in a cell responding to different nutrients. These excess nutrients can lead to important, often detrimental, changes to ecosystems. Even trophic structure in food webs can be influenced by a succession of species dominating the phytoplankton (Anderson et al. 2002).

I addressed questions of both spatial and temporal ecological topology in the IRL by analyzing long-term monitoring data gathered by the state water management districts with a structural equation model (SEM). A relatively complex multivariate conceptual meta model was developed *a priori* (along with more simple models for comparison) that addressed drivers of phytoplankton biomass and the effects of drivers and phytoplankton biomass on selected ecological functions. The first question was whether a single SEM comprised of environmental drivers, phytoplankton biomass, and ecological functions could model the monitoring data gathered from the relatively diverse set of regions and sub-estuaries in the IRL over a long (21 yr) period of time. If so, this would support the idea that a set of variables addressed in environmental monitoring could allow data analyses of proposed cause-and-effect pathways. A sub-question was whether both nitrogen and phosphorus, or just one of these, were important drivers of phytoplankton biomass. Another aspect of this SEM was the importance of the web of indirect effects, individually or in concert as a true 'web.' The second question was whether spatially partitioning the IRL into regions delineated by water residence times, freshwater inputs, and inlets would further increase the model fit of this SEM. Finally, the third question assessed temporal partitioning of long vs. short water residence time regions into periods of the very large blooms (2010–2011) and several previous time periods of the same length to determine whether the causes of increased phytoplankton biomass in the northern estuary could be discerned, as well as the effects of this on ecological functions, and whether the drivers of phytoplankton biomass changed over time. More details on SEM hypotheses are presented in the 'Methods' section.

METHODS

IRL estuary study area

The IRL (Fig. 1) is comprised of 3 major water bodies: the 'Indian River Lagoon proper', which extends from Jupiter Inlet in the south (25° 56.667′ N) past Titusville in the north (up to 28° 47.869′ N); Banana River, which is a semi-enclosed water body east of Titusville and Merritt Island at Cape Canaveral; and Mosquito Lagoon, which lies north of the Cape and culminates at Ponce Inlet (29° 4.584′ N). Mosquito Lagoon is connected to the IRL proper by the very small Haulover Canal (28° 44.222′ N). St. Lucie, Ft. Pierce, and Sebastian Inlets (27° 9.972′ N, 27° 28.312′ N, and 27° 51.630′ N, respectively) are the other 3 main connections with the Atlantic Ocean, and there is a minor connection between Banana River and the Atlantic, with locks limiting water exchange, at Port Canaveral (28° 24.568′ N). All these water bodies are narrow and shallow and typically dominated by seagrass or mudflats subtidally and mangrove or marsh intertidally. Major tributaries including the Loxahatchee, St. Lucie, and Sebastian Rivers were not included in the study.

The IRL was divided into 7 study regions as shown in Fig. 1. Selected physicochemical factors are given for each region in Table 1.

SEM and hypotheses

The overarching hypothesis (or the 'one SEM to rule them all' hypothesis) illustrated in Fig. 2 states that, for the entire IRL and all 21 yr, nutrients, temperature, distance to inlet, and other factors have direct and indirect effects on phytoplankton biomass, which can then influence ecological functions such as changing the dissolved oxygen (DO) and light penetration regimes of the water column.

This hypothesis was posed as a multivariate SEM with a web of paths connecting the biotic and ecological function variables of interest to the other water quality variables and geographic location variables (Fig. 2). In the multivariate hypothesis, chlorophyll *a* (chl *a*; as a proxy for total phytoplankton biomass) and chl *b* and *c* (as proxies for the relative contribution of various major taxonomic groupings) were predicted to respond to a suite of environmental factors in a manner that was consistent throughout the IRL. Chl *a* is contained in all eukaryotic algae, cyanobacteria, and higher plants; chl *b* is found in higher plants, Class Chlorophyta (green algae, prasinophytes, and euglenoids); and chl *c* occurs in Class Bacillario-

Table 1. Long-term (1992–2012) untransformed medians, maximums (for some variables), and coefficients of variation (CV) for chl *a* (mg l^{-1}), total Kjeldahl nitrogen (TKN; µg l^{-1}), total phosphorus (TP, µg l^{-1}), salinity (PSU), and turbidity (NTU). Data in the top row are for the entire Indian River Lagoon (IRL, Florida, USA) while data for the 7 regions are presented individually. All data provided by the St. Johns River Water Management District (northern and central IRL) and the South Florida Water Management District (southern IRL)

Region	Water residence time	Measure	Chl *a*	Max chl *a*	TKN	Max TKN	TP	Max TP	Salinity	Turbidity
All regions combined	Intermed.	Median	4.5	194.6	0.68	6.05	0.052	0.47	28.2	3.8
		CV	1.45	–	0.6	–	0.64	–	0.27	0.08
7 (Mosquito Lagoon)	Long	Median	4.5	194.6	0.65	1.85	0.05	0.29	33.6	5.8
		CV	1.96	–	0.52	–	0.58	–	0.1	0.7
6 (Banana River)	Long	Median	5.4	125.8	1.07	2.25	0.045	0.22	21.9	3.4
		CV	1.38	–	0.24	–	0.56	–	0.3	0.7
5	Long	Median	4.8	168.8	0.95	2.24	0.045	0.3	25.8	3.1
		CV	1.65	–	0.29	–	0.6	–	0.2	0.8
4	Long	Median	4.9	78.6	0.7	2.09	0.055	0.294	22.8	3
		CV	1.13	–	0.33	–	0.49	–	0.1	0.7
3 (IRL proper)	Short	Median	4.8	79.1	0.56	2.08	0.08	0.47	27.8	3.9
		CV	0.97	–	0.46	–	0.54	–	0.2	0.7
2	Short	Median	4	54	0.45	6.05	0.05	0.34	32.1	4.7
		CV	0.94	–	0.95	–	0.59	–	0.2	0.9
1	Short	Median	3.7	53	0.35	1.08	0.033	0.209	32.8	3.7
		CV	0.88	–	1.37	–	0.73	–	0.2	0.6

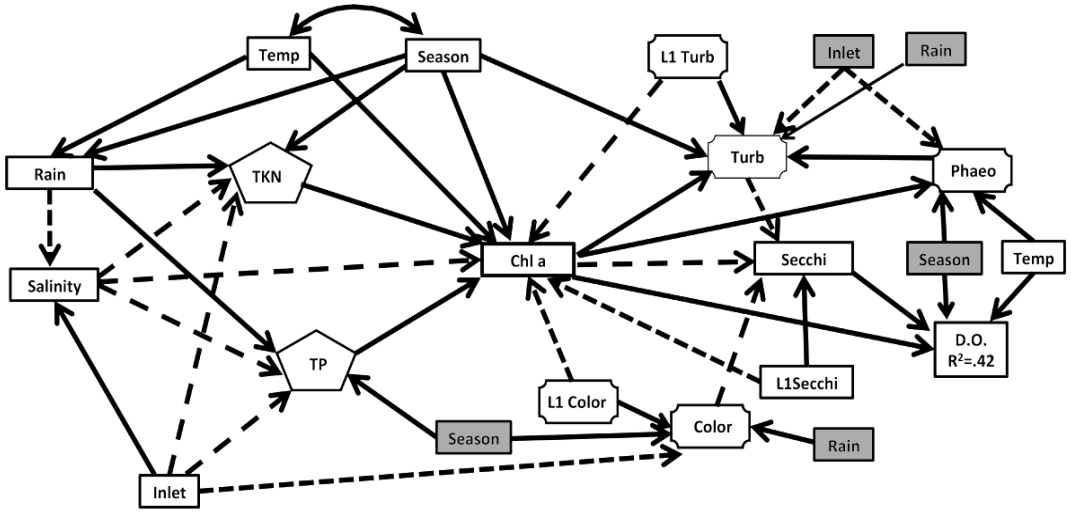

Fig. 2. Full conceptual model shown as a multivariate hypothesis. Solid lines indicate hypothesized + path coefficients and dashed lines indicate hypothesized negative effects. Shaded boxes indicate that a variable is illustrated more than once in the diagram just to reduce diagram clutter that would be caused by crossing or curved lines. All response variables had lags, but most are not shown here to reduce clutter. Lags shown are L1Secchi, L1Color, and L1Turb because these were hypothesized to influence chlorophyll concentrations. The correlation (double-headed arrow) between season and temperature is shown but others are not to avoid clutter. Season was a dummy variable assigned 0 in the dry winter season and 1 in the wet summer season, hence the solid lines indicating greater values hypothesized in summer

phyceae (Diatoms), Class Pyrrophyta (dinoflagellates), and Class Chrysophyceae (including brown tide organisms recently producing a bloom in the IRL).

Phytoplankton biomass was hypothesized to influence certain water quality variables with the biotic effects constituting ecological functions. Specifically, these were model paths through which light penetration and DO were affected by chl *a* directly via light scattering and absorption and indirectly as increasing biomass (chl *a*) caused an increase in turbidity. Additional ecological functions addressed in the SEM were feedback loops: (1) Nutrients→Phytoplankton biomass→Phaeophytin (released by dying cells) →nutrients; and (2) a time-lagged dependent loop such that the time lag (≈1–1.5 mo) of Light penetration in the previous time step→Phytoplankton biomass→Tur-

bidity→Light penetration in the current month of sampling. As mentioned, time lags of all response variables were used to address the autoregressive nature of the long-term data. The null version of this hypothesis is that the covariance structure implied by the pathways proposed in the SEM does not fit the covariance structure in the data. Thus, if the covariance structure of the model is not different from that of the data, then the null is falsified and the SEM as proposed is supported.

Individual regression relationships among variables were developed either based on knowledge gained in the literature, or from discussions with local experts. A path-by-path explanation for each linkage among variables as well as the actual SEM used in statistical analysis (Fig. S1) are shown in Supplement 1 at www.int-res.com/articles/suppl/m569p055_supp.pdf. Several alternative models, some simpler with variables removed and some more complex with additional variables (e.g. fetch, number of causeway/bridge constrictions, size of region, total suspended solids instead of turbidity, etc.) were also tested, but none fit as well as the model selected and are not discussed further in this paper.

This hypothesis was rejected (see 'Results'), leading to the analyses described below.

Specific hypotheses addressed once the null version of the 'one SEM to rule them all' hypothesis was rejected

Hypothesis 1 (the single vs. multiple limiting nutrients hypothesis): *Phytoplankton biomass experienced co-nutrient limitation rather than being affected only by a single nutrient over the scale of the entire IRL estuarine system.* Hypothesis 1 posited that both total Kjeldahl nitrogen (TKN) and total phosphorus (TP) are co-dominant drivers of chl *a* (total phytoplankton biomass) because different taxa could respond to nitrogen or phosphorus. If both total Kjeldahl nitrogen (TKN) and TP are found to be significant drivers of chl *a*, then this supports the hypothesis. Further, if chl *b* and *c* respond differently to TKN and TP, then this also supports the hypothesis. Hypothesis 1 was addressed as part of the analysis of the over-arching SEM described above.

To further test this hypothesis, a 'virtual experiment' was conducted to quantify the nature of responses of phytoplankton biomass to changing nutrient conditions. In this virtual experiment, the SEM was re-run but with selection of different subsets of the nutrient data. These constraints included: (1) low-nutrient treatments created by choosing subsets of data in which TKN and/or TP concentrations were below their first quartile and (2) high-nutrient treatments constituting cases where TKN and/or TP concentrations were above their third quartile. Responses of chl *a*, *b*, and *c* to these nutrient 'manipulations,' termed 'statistical control' by Shipley (2000), were assessed. If higher conditions of both nutrients resulted in greater phytoplankton biomass than the case when just one or the other nutrient was elevated, then the concept of limitation by multiple nutrients is supported.

Hypothesis 2 (the spatial scale hypothesis): *There are differences in drivers (including multiple vs. single nutrients) of chl a, b, and c and ecological functions at a smaller scale (regions of the IRL) compared to the large scale of the entire IRL system.* Hypothesis 2 envisioned that different regions have different drivers of biotic and levels of ecological function response variables depending on the 'local' features of that region. The reasoning behind this hypothesis is that the various regions of the IRL have different water residence times, different numbers of river/canal sets with varying magnitudes of freshwater discharge, and different proximities to inlets and their tidal water inputs. These may influence nutrient concentrations, salinity, turbidity, color, and dominant taxa of phytoplankton (e.g. more marine species presumably nearer inlets, which may be reflected in the relative amounts of chl *b* and *c*).

A 'by-groups' analysis in Mplus, with regions of the IRL as the groups, was used to test this hypothesis. The null version of this hypothesis is falsified if the by-groups model fits the data. If the by-groups model fits the data better than the entire IRL model, as evidenced by a lower value of Akaike's information criterion (AIC), then this is evidence that there are differences among regions of the IRL. In confirmation, this was tested further by constraining some effects to be the same, such as the paths from TKN→Chl *a*, etc., and re-running the SEM to see if an SEM with equal path coefficients in different regions fit the data. If it does not, then this indicates that those path coefficients are really different across regions.

Some major predictions of this hypothesis are as follows: (1) different factors would be more important drivers of chl *a*, *b*, and *c* in different regions, and particularly that TKN would be the sole or primary dominant nutrient affecting phytoplankton in some regions and TP in others; (2) in regions with multiple inlets (e.g. one at each end), salinity might be less variable throughout the region and have less effect on phytoplankton biomass than in regions more isolated from tidal influence; (3) the effects of tempera-

ture and season on phytoplankton may vary because there is a gradient in winter freezes from south to north as evidenced by the transition from mangrove to salt marsh dominance in the intertidal zone; (4) the effects of chl *a* on the ecological functions light penetration and DO should vary among regions in direct proportion to the difference in total phytoplankton biomass in different regions; and (5) temperature should affect DO similarly in all regions, although the effect in northern regions might be stronger in magnitude because of a larger temperature range.

Hypothesis 3 (the temporal scale hypothesis): *There are differences in drivers (including multiple vs. single nutrients) of chl a, b, and c and ecological functions during the timeframe of phytoplankton blooms in the IRL (2010–2011) compared with previous years.* For this SEM, the data were divided into a series of sequential 3 yr groups beginning with the 1992–1994 group and culminating in the 2010–2012 group. A 'by-groups' SEM analysis was carried out on different 3 yr groupings of years for combinations of short residence time (combining Regions 1 to 3) and longer residence time regions (combining Regions 4 to 7), with the primary goal of comparing biotic and ecological functions occurring during the years of large blooms (2010–2012). The reason for the 3 yr groups was that high-intensity phytoplankton blooms occurred over extensive areas of the northern long residence time regions between 2010 and 2012, producing concerns that the northern IRL was in a transition state from benthic to planktonic-dominated primary production. Thus, 2010–2012 was a defining period for temporal SEM analyses, and previous 3 yr groupings were produced in order to facilitate appropriate comparisons.

SEM 'panel model' approach to time-series data

The dataset formed a time series, with sampling ranging between monthly at some sites and 1–3 mo (in some years) at others. The non-independence and autocorrelation inherent in time-series data was handled by using time lags of each response variable as additional regressors (e.g. 'L1Chl*a*→Chl*a*' indicates that the present month's chl *a* is regressed on the previous month's value) in a 'panel model' style analysis (Grace 2006). A preliminary analysis by autoregression was used to identify the order of time lags, and a 1-step time lag (1 mo in some regions and approximately 1.5 mo or slightly less in others) was used for all variables except chl *a*, which was best modeled using both 1- and 2-step time lags.

SEM fit and effect sizes

When the covariance structure implied in the SEM does not differ significantly from the actual covariance structure in the dataset, then the multivariate hypothesis is supported. SEM fit was analyzed using the root mean square error of approximation (RMSEA) instead of chi-squared because of the massive amount of data (Grace 2006, Salewski & Proffitt 2016), and the comparative fit index (CFI) and the Tucker-Lewis index (TLI) were used to test the model for improvement of fit over the baseline model.

All SEM analyses for this study were conducted using the software Mplus (Muthén & Muthén 2010). Here, standardized path coefficients are reported, as these reflect relative importance or effect sizes (Grace 2006). Effect sizes are defined as significant standardized path coefficients of the following ranges in magnitude: small effect, <0.15; moderate effect, 0.15 to <0.25; strong effect 0.25 to <0.35; and very strong effect, ≥ 0.35. Because of the large number of lines of data, many very small effects are statistically significant in these analysis. It is not possible to determine if some effects are too small to be biologically meaningful; however, the standardized path coefficient cutoff of 0.07 was used here. Paths with effect sizes below this are not considered here to be ecologically important and are not shown in SEM results unless they were integral to some longer specific pathway being discussed.

Description of the dataset

The dataset analyzed included 21 yr of data (>10 000 lines of data) gathered from water quality stations ranging from Jupiter Inlet in the south to near Ponce Inlet in the north. One set of stations is monitored by the South Florida Water Management District, and the other set by the St. Johns River Water Management District. Water quality stations within tributary rivers and canals were not included in the analysis. Over the years, times between samplings ranged from 1.0–1.3 mo in northern regions to an average of 2.3 mo in the 2 southernmost regions, where sampling was monthly in the summer and less frequent in the winter. Individual water quality stations in each region were used as replicates in the by-groups analysis, and all stations were replicates in the whole-IRL analysis. In total, data from 76 water quality stations were used. However, in some regions, some stations were discontinued or started

later than others and/or others moved and given a slightly different name, and in these cases they were combined into a single station.

RESULTS

Patterns of chl *a*, *b*, *c*, TKN, TP, and salinity

Chl *a* and *c* concentrations followed similar patterns when regions were compared with all years combined, while chl *b* was substantially lower than chl *a* and *c* in all regions but was particularly low in Regions 1 and 2. If bloom conditions are defined as chl $a \geq 10$ µg l^{-1} (cutoff set following discussions) with phytoplankton experts; see 'Acknowledgments', every region experienced blooms over the study period, although some of the northern regions experienced them far more frequently and some of the regions had blooms during the early years of the study but not later ones. TKN increased from Region 1 to 6, and declined in Region 7. TP was lowest in Region 1 and greatest in Region 3, where the Vero Beach relief canals are known to input considerable amounts of phosphorus (Sigua et al. 2000). Salinity was highest in Regions 1, 2, 3, and 7 (the short residence time regions experiencing the most tidal exchange), and lowest in Regions 4 and 6. Region 4, by the Sebastian River, had the greatest variability (coefficient of variation, CV) of salinity. TKN was much greater in northern, long residence time regions, but there was less difference in TP. Turbidity was substantially greater in Region 7 (Mosquito Lagoon) compared to all other regions. Regions 5, 6, and 7 (long residence time regions) had the greatest CV of chl *a* over the 21 yr period. All long residence time regions (4–7) had maximum chl *a* values greater than any seen in the short residence time regions.

Relationships of chl *a* to TKN and TP by region

Chl *a* increased with both increasing TKN and TP in all regions (Fig. 3) and typically reached higher concentrations in the wet summer season. Lowest values, and the least clear response of chl *a*, occurred in Region 2 (St. Lucie Inlet to Ft. Pierce Inlet), and highest values in Regions 6 (Banana River) and 7 (Mosquito Lagoon). In many regions, and especially in the summer, the changing slopes of the arrow vectors in Fig. 3 implied that increases in chl *a* with TP were beginning to level off, meaning little further increase in chl *a* with additional change in TP. This suggested a quadratic relationship between chl *a* and TP, so a TP-squared term (TP^2) was introduced into the SEM (see next section). A quadratic relationship for TKN was tested as well but did not fit the data and was therefore not included in the best SEM.

Multivariate hypothesis testing with SEM

The SEM of the causal and correlative arrangement of paths of all biotic and environmental variables falsified the null version of the over-arching (one model to rule them all) hypothesis, since the covariance structure implied by the model fit that of the data well (RMSEA = 0.049 [90% CI 0.048–0.051], p = 0.835; CFI = 0.946, TLI = 0.913, AIC = 1089036, number of freely estimated parameters = 299, N = 10 514). This supports the idea that changes in biotic variables (chl *a*, *b*, *c*, and phaeophytin, a chlorophyll breakdown product) and ecological functions (Secchi depth, DO, and feedback loops) were influenced by a suite of physical factors including nutrients, light penetration (Secchi depth, turbidity, and color), salinity, rainfall, and location relative to inlets (Fig. 4 and the entire SEM in Fig. S2 in Supplement 2). For chl *a*, $R^2 = 0.46$. Thus, about half of the variance in chl *a* over a long-term and large spatial scale was explained by the SEM posed as the multivariate hypothesis. The remaining variability in chl *a* was likely produced by other physical and biotic variables.

Chl *a* increased with increases in both TKN and TP, although the effect size (i.e. the standardized path coefficient) was greater for TP (Figs. 4A & S2). The quadratic TP^2 term was significant and the effect on chl *a* was negative, which confirmed the graph observation of the existence that a threshold exists for the effect of TP on chl *a*. Other factors, season, temperature, and salinity had small positive effects on chl *a*. The positive effect of season means that chl *a* was higher in the summer wet season (dummy variable coded 1) compared to the winter, dry season (dummy coded 0).

Chl *b* and *c* were analyzed in the same SEM with chl *a* but are not shown in figures to reduce clutter. Instead, direct coefficients are given in Table S1 in Supplement 3. The amount of variation explained for both chl *b* ($R^2 = 0.14$) and chl *c* ($R^2 = 0.31$) was less than that for chl *a* ($R^2 = 0.46$). Chl *c* responded to the set of predictor variables in very similar fashion to that noted above for chl *a* (Table S1, Fig. 4A), although the effects of both nutrients were reduced and the effects of season, while small and positive for

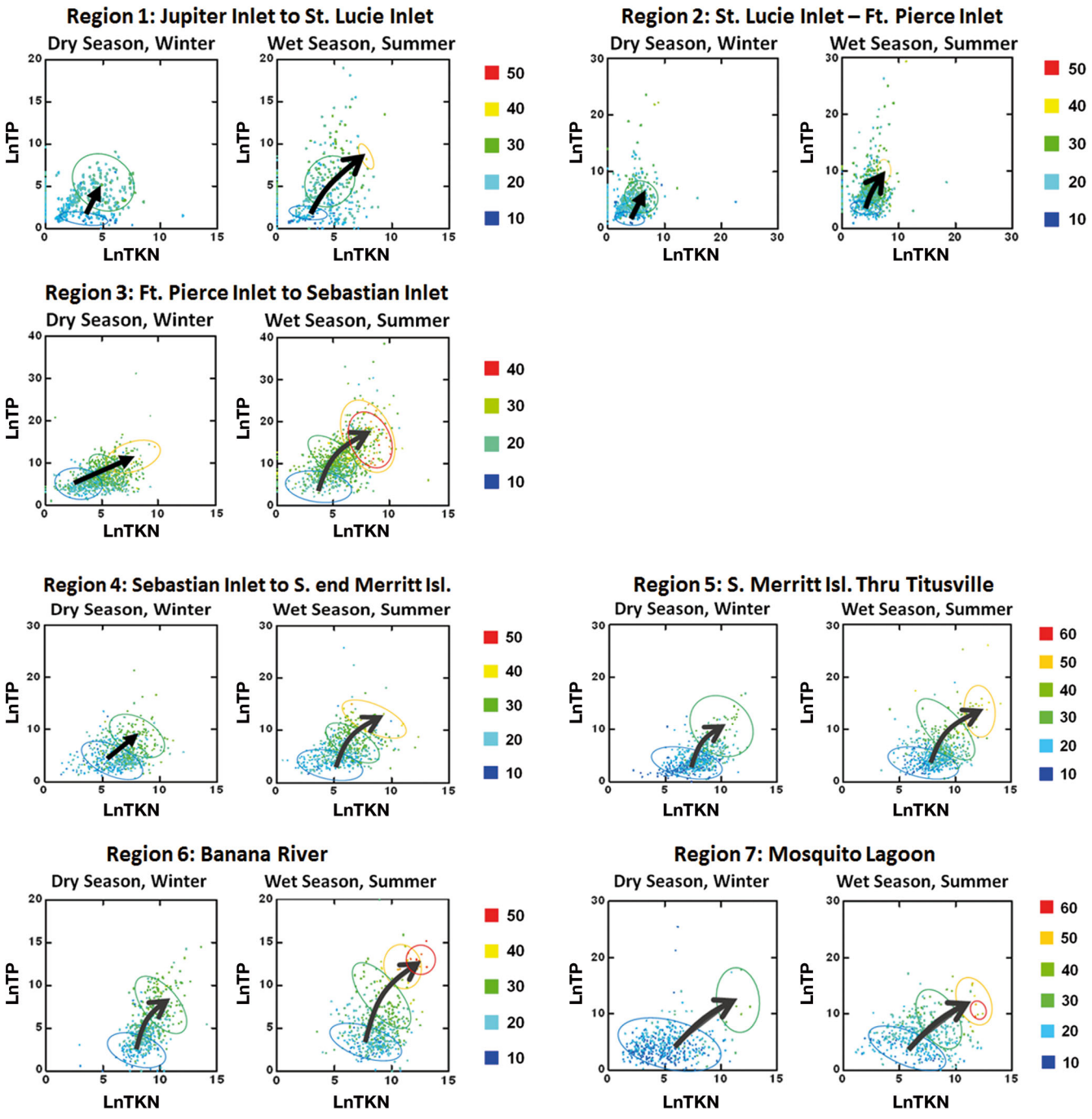

Fig. 3. Relationships of chl *a* (*z*-axis, represented by colors) as a function of total Kjeldahl nitrogen (TKN; *x*-axis) and total phosphorus (TP; *y*-axis) are illustrated for Indian River Lagoon (IRL) Regions 1 to 3 (top 3 graphs), the short residence time regions; and Regions 4 to 7 (bottom 4 graphs), the longer residence time regions. Ovals illustrate the areas of lower concentrations of chl *a* (blue and green) to higher (gold) and highest (red) concentrations. The arrow indicates the trajectory of increasing chl *a* as nitrogen and phosphorus increase. Points are from each water quality station and cover all time periods. All variables are ln-transformed. TKN and chl *a* were multiplied by 10, and TP by 100, after transformation

chl *a*, were not significant for chl *c*. This similarity in response to drivers led to a high correlation (r = 0.71) between chl *a* and *c* (inset box in Fig. S2). Chl *b* responded weakly to both TKN and TP and negatively to season, indicating greater concentrations in winter dry seasons when averaged over all years and regions (Table S1 in Supplement 3). Chl *b* and *c* were moderately correlated (r = 0.25), and there was a rel-

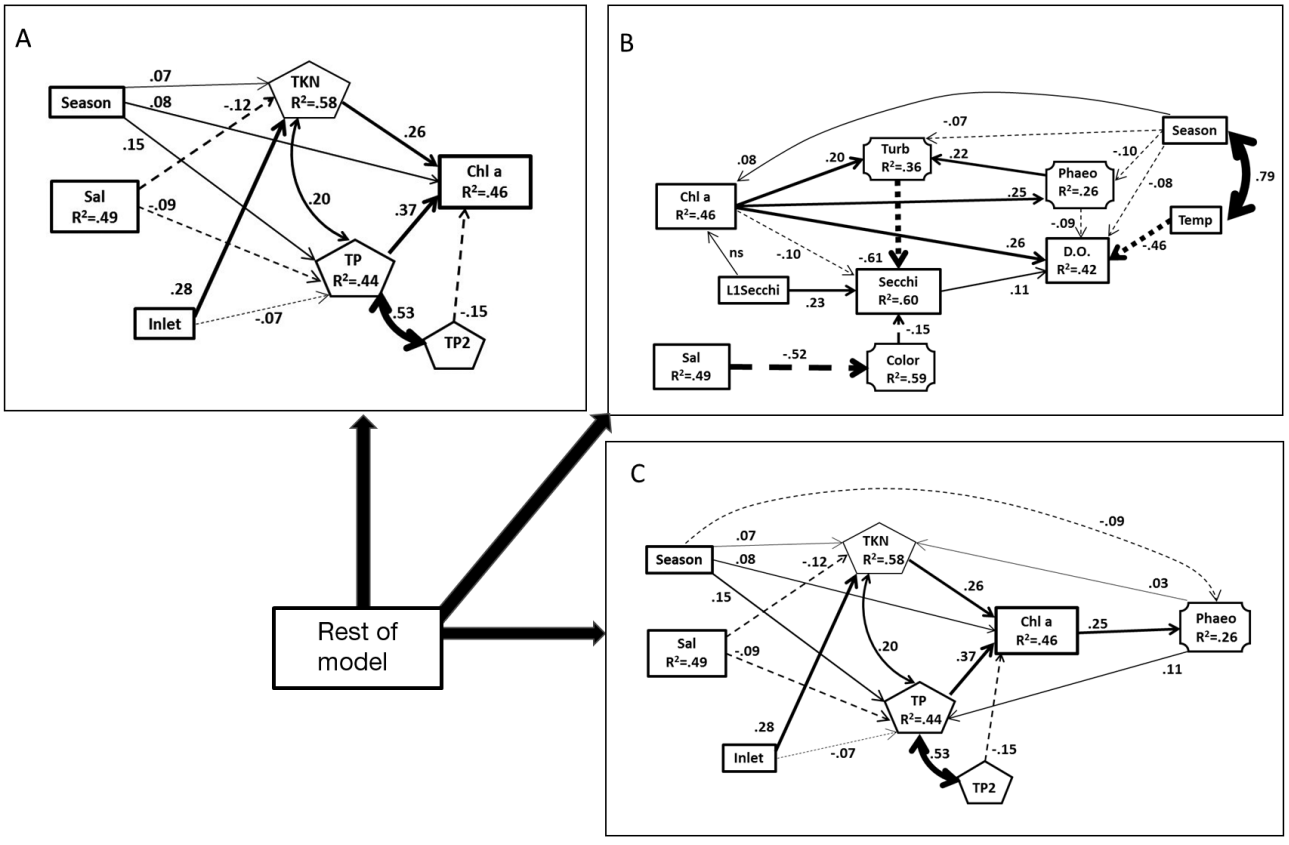

Fig. 4. Sections of the structural equation model (SEM; the entire model is shown in Fig. S2 in the Supplement) focusing on specific points. Except where otherwise noted, lag variables are not shown to reduce clutter. (A) Major factors (nutrients, season, inlet) affecting chl *a*. (B) Section of the SEM showing paths among chl *a*, turbidity (Turb), phaeophytin (Phaeo), dissolved oxygen (DO), salinity (Sal), color, temperature (Temp), and Season. Lag of Secchi depth (L1 Secchi) is included because it is involved in the feedback loop involving light and chl *a*. (C) Feedback loop from chl *a* to Phaeo to TKN and TP, and from the nutrients back to chl *a*. Values on lines are standardized path coefficients

atively low, but significant, correlation between chl *a* and *b* (r = 0.14).

Salinity can affect the composition of phytoplankton by directly selecting for species that tolerate different local, or fluctuating, conditions. Also, increased salinity can indicate dilution of chl *a* and elevated nutrients in estuarine waters by tidal water inputs. I therefore hypothesized that salinity would have considerable importance in chl *a*, *b*, and/or *c* concentrations. However, for all regions of the IRL and years combined, direct, indirect, and total effects of salinity on chl *a* and *c*, while significant, were far below the cutoff in the path coefficient of 0.07 used here, and there were no significant effects on chl *b*.

The biotic variable chl *a* influenced ecological functions of light penetration (via paths involving Secchi depth, phaeophytin, and turbidity) and DO (Fig. 4B). Turbidity increased in response to chl *a* because phytoplankton cells are a component of turbidity. Turbidity also increased as phaeophytin increased (dead lysing cells are also a component of turbidity), and because phaeophytin was also a function of chl *a*, the total effect of chl *a* on turbidity is the sum of the direct (path coefficient = 0.20) and indirect (0.25 × 0.22) effects, yielding 0.26, a large magnitude total effect of Chl*a*→Turb (Fig. 4B). Light penetration (using the proxy variable Secchi disk depth) was negatively affected by turbidity, color, and chl *a*. Chl *a* had a direct effect of −0.10 but a large (−0.26) total negative effect through the 2 indirect paths of Chl*a*→Turb→Secchi and Chl*a*→Phaeo→Turb→Secchi. Salinity, as a proxy for tidal water inputs, had a small (0.09) positive total effect on light penetration largely because of its strong diluting effect on color but also a host of other small indirect effect pathways (Figs. 4B & S2). Salinity had no significant diluting effect on turbidity.

Phytoplankton increased DO by releasing oxygen during photosynthesis (0.26 direct large effect of chl *a* on DO). In contrast, negative indirect effects of

chl *a* on DO through paths involving turbidity, phaeophytin, and Secchi depth reduced the total effect of chl *a* on DO to 0.21, a moderate effect size. Increasing water clarity, indicated by increasing Secchi depth, had a small positive effect on DO as well (direct effect = 0.11), which may be a representation of net photosynthesis by benthic flora (e.g. seagrass, macroalgae, and epiphytes) increasing with water clarity (Fig. 4B). The strongest effect on DO was the negative effect of increasing temperature on DO (direct effect −0.46, a very strong effect).

The other ecological functions included the feedback loops involving nutrients driving phytoplankton, which during decay following cell death re-releases nutrients. In one loop (TP→Chl*a*→Phaeo→TP), phosphorus was a dominant driver of chl *a* which, in turn, influenced the concentration of phaeophytin since it is a breakdown product of chl *a*. Subsequently, phaeophytin positively affected TP concentrations likely through release of inorganic nutrients via decomposition during cell decay (Fig. 4C). The analogous hypothesized loop for nitrogen did not occur when averaged over all regions and years because the effect of phaeophytin on TKN was not significant.

The other feedback loop hypothesized was the effects of the previous month's light penetration (L1Secchi, L1Turb, and L1Color) on the current month's chl *a*, coupled to the current month's chl *a* affecting the current month's turbidity and Secchi. The SEM results did not strongly support the importance of this loop because two of the components (the lags of Secchi and turbidity) had little or no effect on chl *a* (Fig. S2). This may indicate that a month is too long a period between sampling to pick up the effects of reduced light.

SEM virtual experiment: testing the effects on chl *a*, *b*, and *c* of manipulating concentrations of nitrogen and phosphorus

Additional runs of the SEM selected different combinations of nutrient concentrations as 'treatments' and observed the response of biotic (chl *a*, *b*, and *c*) and ecological function (Secchi depth and DO) variables. 'Low' TKN and TP treatments were concentrations less than their first respective quartiles (Q1), and 'high' TKN and TP were values greater than their third quartiles (Q3). The SEM involving different subsets of the data for these variables is shown for low and high nutrient concentrations in Fig. 5, where only part of the SEM is presented for clarity; the rest is indicated by the circle with 'rest of model' inscribed in it. However, the actual model tested had all the same variables and paths as that shown in Fig. S2.

The results of the virtual experiment are compared in Fig. 5. Fig. 5A presents the case using all values of TKN and TP. When both TKN and TP were constrained to be low (below their Q1 levels), TP was the sole nutrient driver of chl *a* while TKN was the sole driver of chl *b* (Fig. 5B). Under low TKN and TP nutrient conditions (Fig. 5B) the correlations between chl *a*, *b*, and *c* were reduced relative to the condition when all levels of nutrients were allowed (Fig. 5A). Higher levels of chl *a* and *c* caused increases in phaeophytin, which affected turbidity and light penetration, and chl *a* had direct positive effects on turbidity and negative effects on Secchi depth (direct = −0.15, total = −0.29). However, there was no significant effect of light penetration (Secchi) on DO (Fig. 5), nor did chl *a* have any direct effect on DO under low TKN and low TKN+TP scenarios. This likely means that at low levels of both nutrients, the resulting chl *a* was not sufficiently high enough to reduce light penetration, or to have a net positive contribution to DO directly via evolution of oxygen during photosynthesis, and consequently DO values were reflecting primarily benthic net photosynthesis.

When TKN was held low and TP allowed to vary naturally, TP became the dominant driver of chl *a* and *c*, although TKN still affected chl *b* (Fig. 5C). The apparent negative effect of TKN on chl *c* was probably reflecting consumption of TKN by phytoplankton producing even lower levels, in other words, the direction of the causal arrow might be reversed in this case.

At high nutrient levels (either or both TKN and TP > Q3 levels, Fig. 5E–G) the dominant nutrient driver of chl *a* was TP when TKN was high (Fig. 5E) and TKN when TP was high, as would be expected from limiting nutrient theory (Fig. 5F). When both nutrients were in high concentrations (Fig. 5G), the driver of chl *a* was mainly TKN, possibly because the effects of TP were leveling off as indicated by the significant quadratic effect discussed earlier, although not specifically illustrated in Fig. 5. Drivers for chl *c* were similar to those of chl *a*, not surprisingly, since chl *a* and *c* were highly positively correlated at high TKN and high TKN+TP concentrations, although not at just high TP levels (Fig. 5). However, at high nutrient levels, chl *b* responded mainly to increasing TP and temperature and never to TKN. There were the expected effects of elevated chlorophylls on phaeophytin and turbidity and Secchi disk depth. At high nutrient conditions, the resulting high chl *a* produced

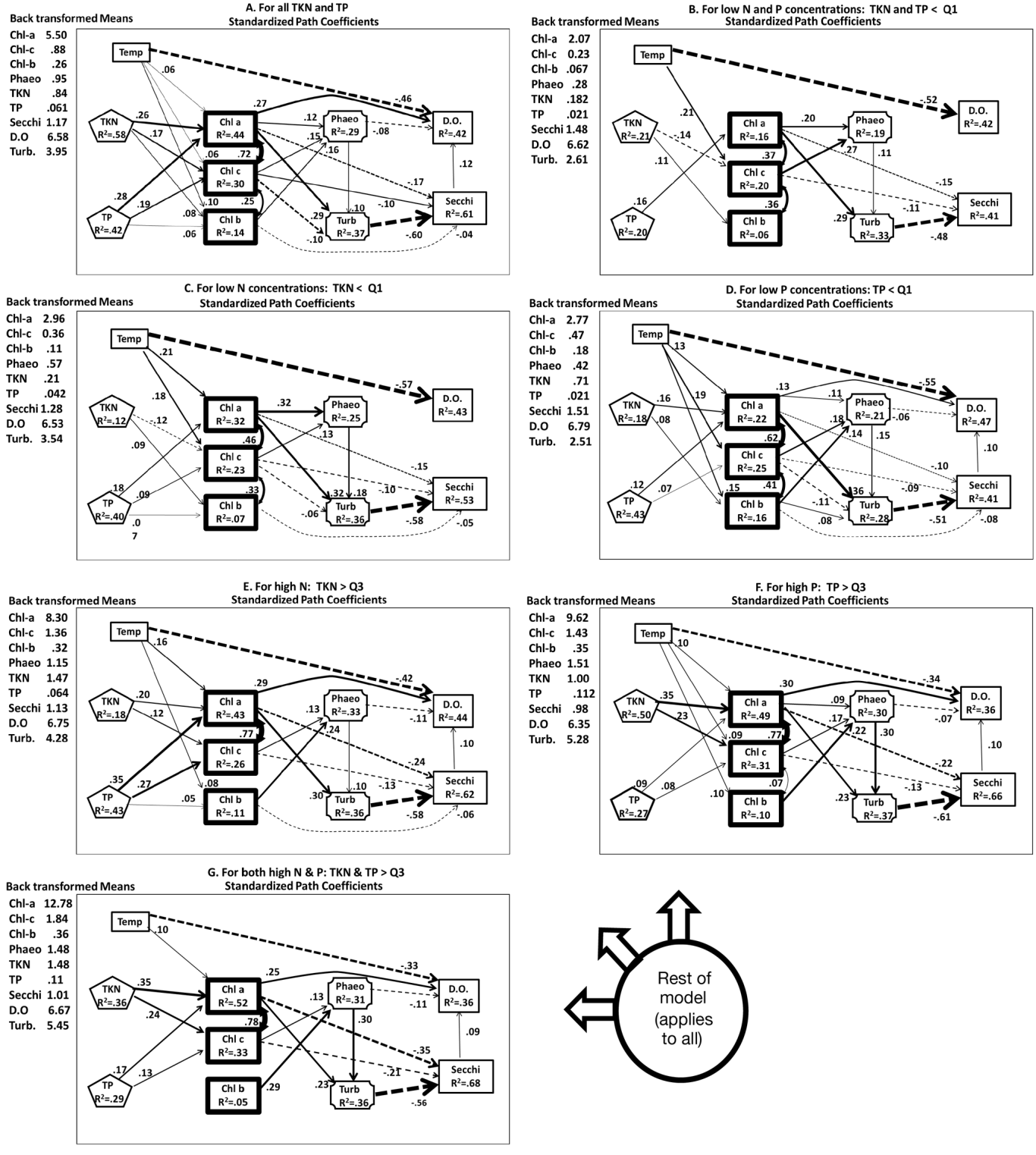

Fig. 5. Subset of the variables analyzed, displayed for the following cases: (A) all levels of TKN and TP as primary drivers of chl *a*, *b*, and *c*; (B) when only values of TKN < its first quartile are selected; (C) when only values of TP < its first quartile are used; (D) when both TKN and TP are < their first quartile; (E) when TKN > third quartile and TP varies naturally; (F) when TP > third quartile and TKN varies naturally; and (G) both TKN and TP are above their third quartile. The remainder of the model shown in Fig. 4 is represented by the circle labeled 'Rest of model.' Standardized path coefficients and back-transformed means for each variable are shown. All regions and all years are combined here

a strong positive effect on DO, as well as some negative indirect effects. Further, at high concentrations of nutrients and chl *a*, there was a significant, although small in magnitude, effect of increasing Secchi depth on DO (Fig. 5E–G). This suggested that chl *a* can reduce DO somewhat by restricting light penetration to the benthic primary producers. In other words, when chl *a* was lower than its average value for high nutrients, and thus Secchi depth was greater, DO increased because more light is reaching the benthic plant assemblage.

Testing the regional hypothesis (Hypothesis 2)

Hypothesis 2 predicted that when the IRL was subdivided into smaller spatial scale 'regions,' phytoplankton biomass would have different drivers in different regions and the overall SEM would fit the data better than the 'entire IRL' model. Partitioning the IRL into regions in a 'by-group' analysis in Mplus provided a better overall model fit in terms of AIC than did analyzing the IRL as a single entity (by regions, AIC = 1 013 513, compared to the entire IRL, AIC = 1 088 515). However, other measures of model fit for the by-regions model (RMSEA = 0.06, $p < 0.005$, CFI = 0.918, and TLI = 0.87) were not quite as good as that for the entire IRL analyzed together. Part of the SEM is shown for each region in Fig. 6 and Table 2, although simply to save space, Fig. 6 does not have the circle with 'rest of model' inscribed as was done in Fig. 5. SEM results by region for all response variables are presented in Table S2 in Supplement 4.

Table 2. Standardized direct path coefficients for response variables chl *b* and *c*, to accompany the chl *a* results shown in Fig. 6. The response variable is given in bold (with its R^2 value) above various predictor variables with standardized coefficients, standard errors, and p-values

	Standardized coefficient	SE	p
Chl *b* (R^2 = 0.14)			
L1CHLB	0.300	0.011	0.000
TN	0.082	0.014	0.000
TP	0.114	0.014	0.000
TP2	−0.064	0.013	0.000
TEMP	0.088	0.016	0.000
L1COLOR	0.003	0.014	0.819
L1SECCHI	−0.052	0.017	0.002
SALINITY	−0.001	0.012	0.922
DIST_INL	0.070	0.014	0.000
L1TURB	−0.063	0.016	0.000
SEASON01	−0.125	0.016	0.000
Chl *c* (R^2 = 0.31)			
L1CHLC	0.368	0.008	0.000
TN	0.168	0.013	0.000
TP	0.279	0.013	0.000
TP2	−0.114	0.012	0.000
TEMP	0.056	0.014	0.000
L1COLOR	−0.042	0.012	0.000
L1SECCHI	0.030	0.015	0.042
SALINITY	0.029	0.011	0.007
DIST_INL	0.074	0.012	0.000
L1TURB	−0.058	0.014	0.000
SEASON01	0.014	0.014	0.346

Biotic response variables

Both TKN and TP were significant drivers of chl *a* in all regions except Region 2, where there was no effect of TKN (Fig. 6). However, the relative magnitudes of path coefficients varied considerably among the 6 regions where there were co-limitations of nutrients. TP was usually the strongest driver of chl *a*, although TP and TKN were similar in effect size (here, standardized path coefficients) in Regions 1, 4, and 7. In most regions, temperature and salinity had small positive effect sizes on chl *a*, if any. However, in Region 2 (St. Lucie Inlet – Ft. Pierce Inlet), there was a strong negative direct effect (–0.31) of salinity on chl *a* (Fig. 6C). To further confirm that TKN and TP had different effects in different regions, the path coefficients TKN→Chl*a* and TP→Chl*a* were tested for significance by constraining them to be equal among regions in the Mplus program and then re-running the model. SEM runs with path coefficients constrained to be equal across regions did not fit the data using any of the metrics of model fit, which shows that the path coefficients were indeed different (Grace 2006).

Chl *c* was highly correlated with chl *a*, ranging from r = 0.63 to 0.80 in all regions except Region 2, where the correlation was substantially lower (r = 0.49). Where chl *a* and *c* were highly correlated, the responses to nutrients were similar to that discussed above for chl *a*. In Region 2, where the correlation between chl *a* and *c* was the lowest, TP did not affect chl *c* at all, and TKN had a small negative effect, suggesting that phytoplankton are consuming TKN down to limiting concentrations (Fig. 6C).

In long residence time regions, chl *b* did not respond to TP and was affected by TKN only in Region 4 (Fig. 6D–G). However, chl *b* was always

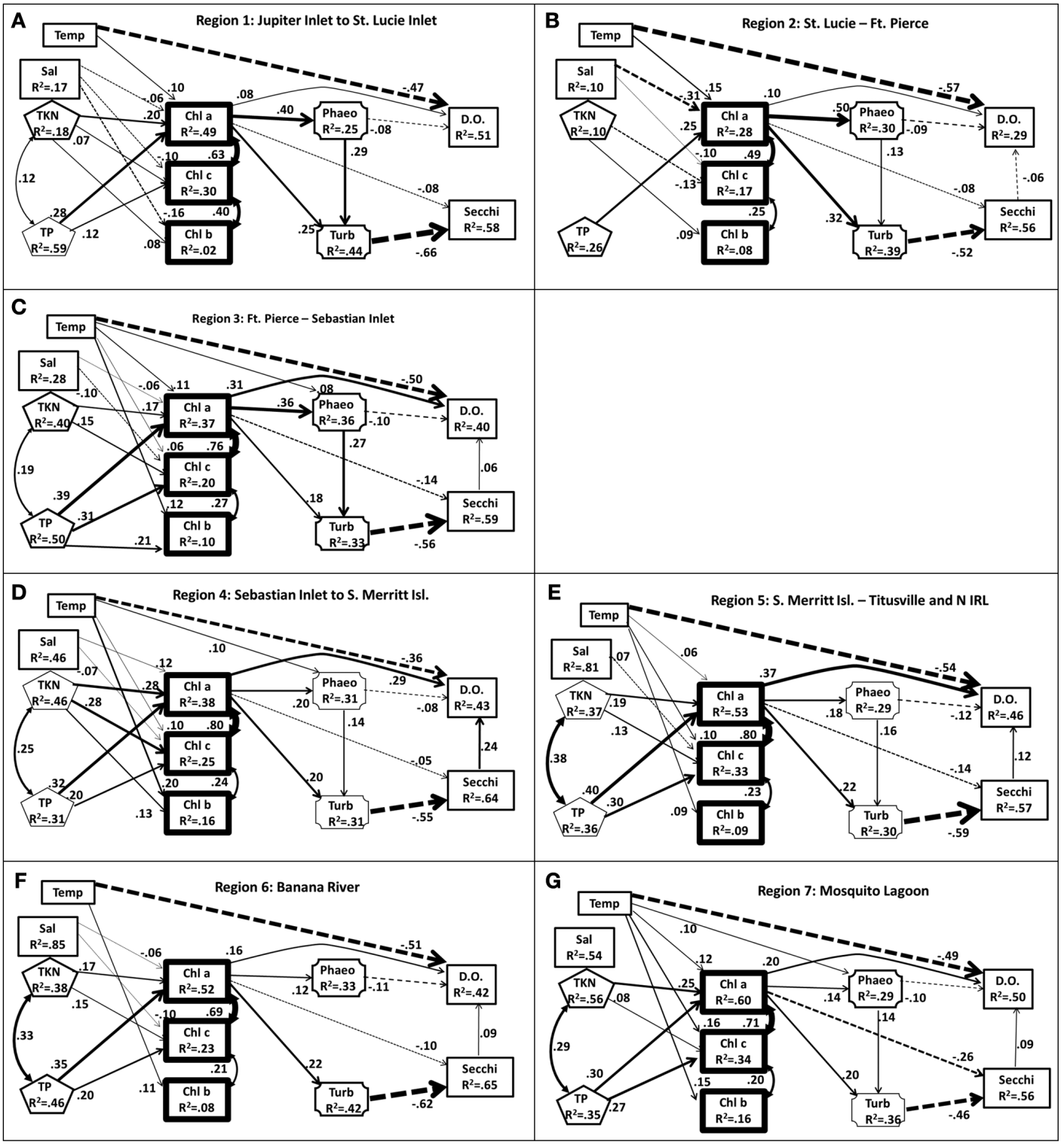

Fig. 6. Subset of the structural equation model (SEM) results by the 7 regions for all years are given here for (A–C) regions with short water residence times and (D–G) regions with longer residence times. For each region, all years are included. A circle labeled 'Rest of model' (depicted in Figs. 7 & 8) is not reproduced here to save space, but should be understood as present. Standardized path coefficients are shown. All data were log transformed before analyses. For the 'by-regions' Mplus analysis, model fit values are: root mean square error of approximation = 0.060, comparative fit index = 0.918, Tucker-Lewis index = 0.87, Akaike's information criterion = 1 014 115, number of free parameters = 2065. N for each region: Region 1 (panel A) = 986, 2 = 1570, 3 = 2127, 4 = 1579, 5 = 1770, 6 = 1424, and 7 (panel G) = 1058

positively influenced by increasing temperatures, although the effect size was small to moderate depending on region. Changes in salinity had no effect on chl *b* levels in any region except Region 1, where there was a moderate negative effect.

Ecological functions

Chl *a* had direct positive effects on DO in all regions, although the magnitudes varied considerably (standardized path coefficients: from 0.08 [significant but very small] in Region 1, to a very strong 0.37 in Region 5). Temperature was the dominant controller of DO in all regions with very strong negative effects (Fig. 6). Increasing Secchi depth had small to moderate positive effects on DO in all long residence time regions (Fig. 6D–G), but only a small positive effect in 1 short residence time region and an unanticipated very small negative effect in Region 2. Phaeophytin had weak direct negative effects on DO in all regions (Fig. 6).

Turbidity was the primary driver of light penetration (Secchi disk depth) and produced very strong effects in all regions. Chl *a* also had direct negative effects on Secchi depth in all regions, although these varied considerably in magnitude, with the greatest effect occurring in Region 7 (Mosquito Lagoon; Fig. 6). Chl *a* had moderate to strong direct positive effects on turbidity in all regions. Phaeophytin had direct positive effects on turbidity in all regions except Region 6 (Banana River) and thus indirect effects on Secchi disk depth (Fig. 6).

The total effects (the sum of the direct and indirect effects) of chl *a* on the ecological functions Secchi depth and DO also varied by region. In Mosquito Lagoon (Region 7), for example, the total effects of chl *a* on Secchi depth were the sum of the strong direct effects (–0.26) and the indirect paths ([0.14 × 0.14 × –0.46] + [0.20 × –0.46]), which yielded a very strong total effect of –0.36. In Regions 1 to 4, where direct effects of chl *a* on Secchi depth were very weak (–0.05), indirect effects dominated the total effect, for example –0.13 in Region 4.

Testing Hypothesis 3: temporal analysis of changes during the 'bloom years' (2010–2012) compared to previous years

Long residence time and short residence time regions exhibited different trajectories in ecological variables over the course of 2 decades, and the changes in mean chlorophyll concentrations, turbidity, and Secchi depth were mirrored by differences in changes in nutrient drivers (Fig. 7). The mean (±1 SE) values of chl *a* are shown for the combined short residence times regions and combined long residence times regions (bottom graphs) and the standardized TKN and TP effects on the top graphs (Fig. 7). In short residence time regions, mean chl *a* generally declined over time (Fig. 7, bottom left), and the dominant nutrient driver was TP, until about 2008 (midpoint year of the 2007–2009 period) when TP and TKN became co-dominant in effect size (Fig. 7, top left). In long residence time regions, mean chl *a* showed a cycle of moderate increases followed by moderate decreases (Fig. 7, bottom right), until a big jump in the last time group (2010–2012). This spike in mean chl *a* concentration was mirrored by a peak in TKN effect size as well as demarking the first time TKN had been the dominant driver relative to TP (Fig. 7, top right).

In Fig. 8, the effects of the partial model (i.e. nutrients, pigments, and light penetration variables only), are shown for four 3 yr time periods (including 2010–2012, the period with large blooms) for short and long residence time combinations of regions. In the short residence time regions, chl *c* responded in similar fashion as chl *a* to nutrient drivers, shifting from TP dominated in the early years to TKN dominated in middle years, and TKN and TP being co-dominant during the 2010–2012 period, although the magnitude of the TP effects was essentially 2× as strong as that of TKN (Fig. 8A–D). Chl *b* followed a similar pattern except that the magnitude of effects in the later years (2010–2012) was about the same for TP and TKN. In long residence time regions, chl *c* and *a* were highly positively correlated in all year groups (r range: 0.66 to 0.80), and consequently the pattern for chl *c* was similar to the response of chl *a* to nutrient regimes. Percent variation explained for both chl *a* and *c* was greatest during the bloom years (see R^2 values in Fig. 8H). There was little to no effect of TP on chl *b* in the early groups of years, but a relatively strong response during the bloom years of 2010–2012 (Fig. 8E–H). However, the percent variability explained in chl *b* declined from 0.63 in the early year group to <0.13 in all later year groups, suggesting that other factors not included in the SEM are influencing chl *b*.

In short residence time regions, Secchi disk depth was most affected by turbidity, which in turn was a function of phaeophytin or chl *a* or both (Fig. 8A–D). DO was a function of chl *a*, but never Secchi disk depth, which suggests light was not limiting benthic

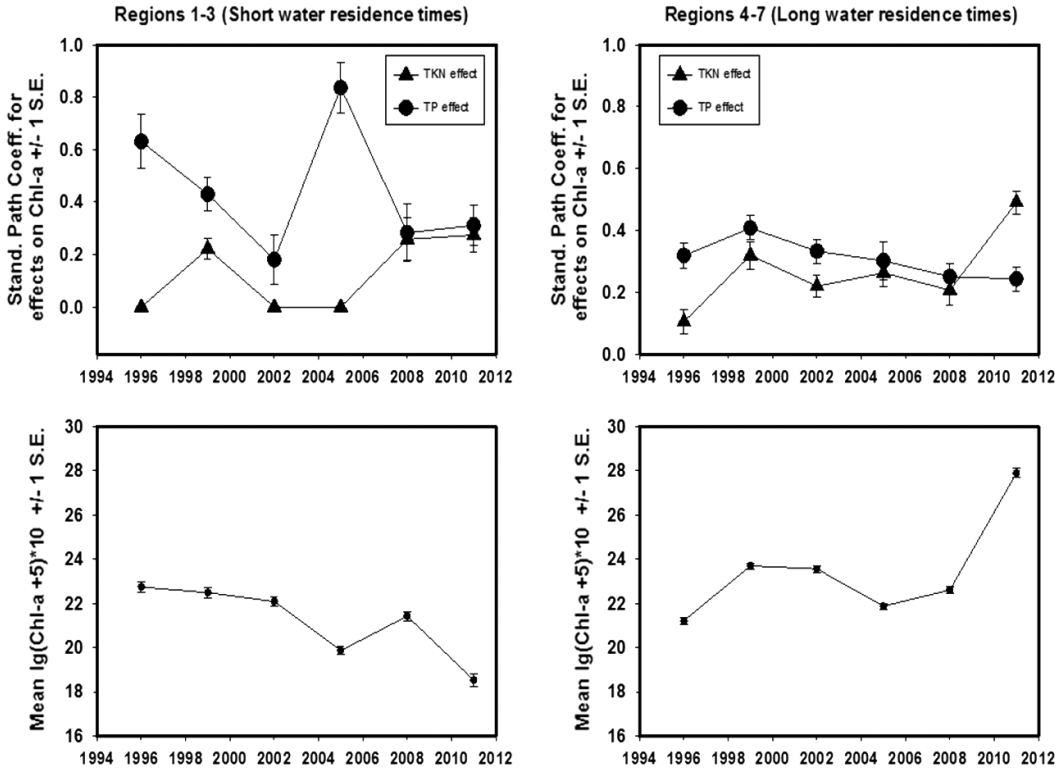

Fig. 7. TKN and TP standardized path coefficients (top graphs) for short water residence time Regions 1 to 3 (panels on left) and long residence time Regions 4 to 7 (panels on right) are plotted against the mid-point of 3 yr groupings. Bottom graphs show the mean ± 1 SE for the same temporal and spatial groupings

photosynthesis in Regions 1 to 3 most of the time. In long residence time regions, turbidity was in part a function of chl *a* and phaeophytin, Secchi depth was a function of turbidity at all times and also of chl *a* directly in the last set of years (Fig. 8E–H). During the bloom years (2010–2012), these variables explained 83% of the variance in Secchi disk depth (Fig. 8H). In 3 of the 4 year groupings (but not the 2010–2012 group), DO was directly affected by chl *a* and Secchi depth.

DISCUSSION

Physical and water quality variables in the IRL were found to be linked in a complex structural equation model that adequately explained a substantial portion of the variance in phytoplankton biomass and ecological functions regardless of regional differences. This suggests that many, or all, of the processes and proposed causal pathways included in the SEM constitute a general finding that may apply to subtropical, and perhaps other, estuaries more broadly. Indirect effects, and small-magnitude direct effects, were important as a group, even though individually their effect sizes were usually quite small. This is consistent with the findings of Hanki (2011), who noted the existence and importance of small-magnitude indirect effects in the extinction of bivalves.

Even though the SEM for the entire IRL fit the data, accounting for regional differences in water residence times and freshwater inflows provided an even better model fit. This improvement was expected, because it accounts for regional differences in water residence times known to be a highly important environmental factor affecting a number of variables. Furthermore, when the superbloom and other large bloom years were compared to previous years for groups of long and short residence time regions, it became clear that the dominant environmental drivers changed over time and this, at least in part, was responsible for the huge blooms between 2010 and 2012 in the northern, longer residence time, regions.

Single vs. multiple nutrient limitation

Clearly, nutrients are key factors in the ecology of the IRL and many other estuaries. Increasing concen-

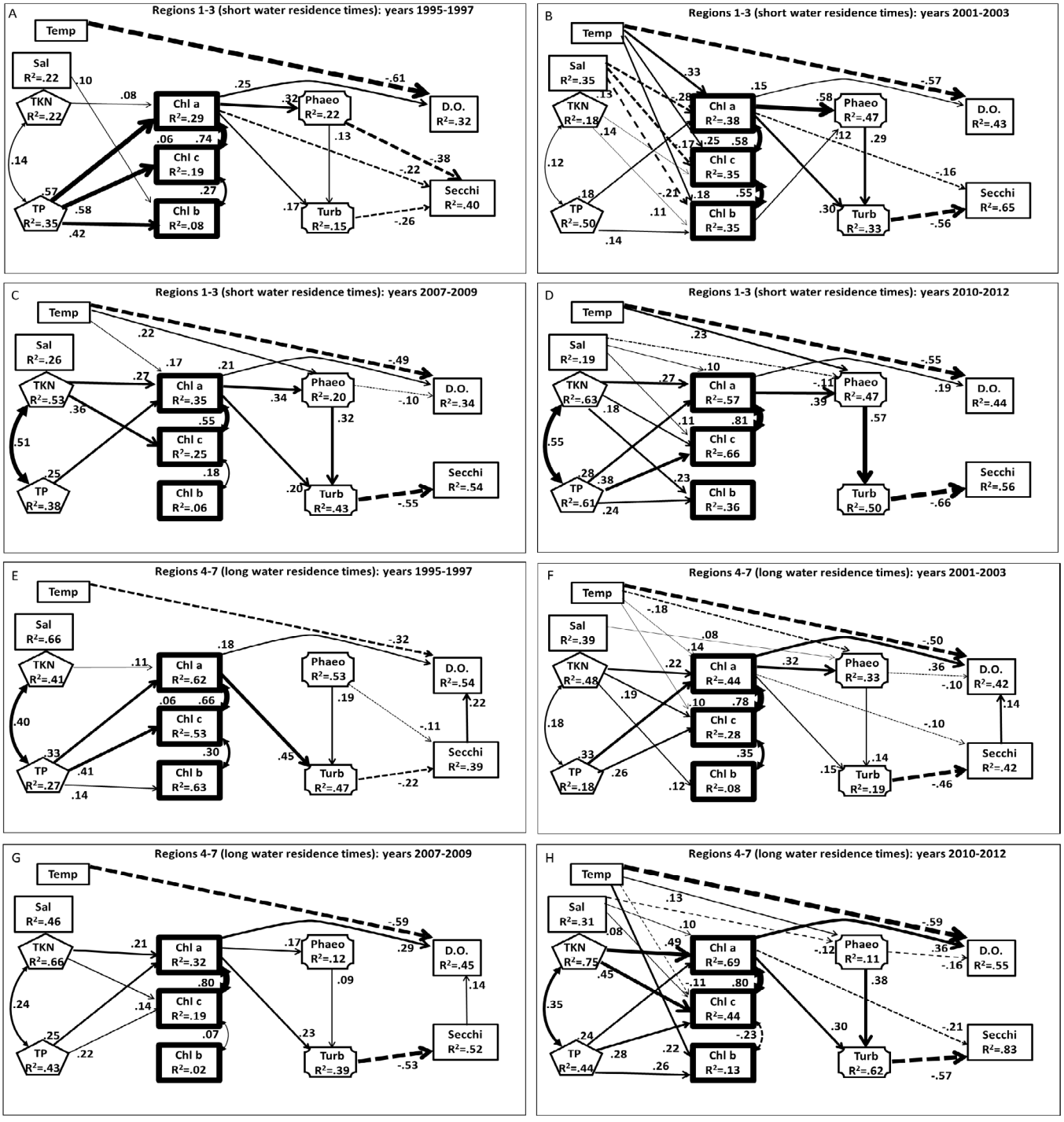

Fig. 8. Sections of the structural equation model (SEM) by short (Regions 1 to 3) and long water residence times (Regions 4 to 7) for four 3 yr groupings culminating in the 2010–2012 period in which the blooms in the northern regions occurred

trations over the years constitute a disturbance to the system. The SEM analyses here support the idea that multiple nutrients, e.g. nitrogen and phosphorus in the case of the IRL, can be co-limiting and that changes in the absolute and relative concentrations of nutrients can produce important differences in phytoplankton biomass and dominance. The IRL SEM analyses indicated that both TKN (N) and TP (P) were important drivers of phytoplankton biomass (chl *a*, *b*, and *c*), although phosphorus showed a threshold above which increasing phosphorus produced little or no further increases in chl *a*. Nutrient

co-limitation findings are consistent with the findings of Whitehouse & LaPointe (2015), who reported that simple N:P ratios are not sufficient to understand macroalgal blooms in the IRL, and Salewski & Proffitt (2016), who found limitation of chl *a* by both nitrogen and phosphorus over a 10 yr period in the St. Lucie River estuary, a tributary of the IRL. Mallin et al. (1999) found nutrient co-limitation at times, and alternating between nitrogen and phosphorus limitation at other points in a North Carolina estuary. Nielsen et al. (2002) reported that nitrogen was a leading driver of phytoplankton in Danish coastal waters. Anderson et al. (2002) noted in a review that both nitrogen and phosphorus could co-limit phytoplankton growth and that silicon and iron could affect the phytoplankton dominance suite. Worldwide, phytoplankton biomass (chl *a*) has been linked to total nitrogen and phosphorus concentrations (Smith 2006), although in some highly turbid estuaries, light limitation can predominate over nutrient effects (Pennock & Sharp 1994). In systems with high freshwater water flow rates, the effects of nutrients can be reduced (Arhonditsis et al. 2007). Malone et al. (1996) reported that dissolved silicate was also important, along with dissolved inorganic forms of nitrogen and phosphorus depending on season. Similarly, in a southwestern Iberian estuary, high N:P ratios and abundant silicon were drivers of phytoplankton. In China's Pearl River estuary, Yin et al. (2000) suggested that phosphorus and silicon were co-limiting phytoplankton. Yin (2002) reported that phosphorus was an important limiting factor in waters near Hong Kong but that seasonal influences were affected by monsoons.

In the context of disturbance ecology: linking phytoplankton biomass to seagrass loss

Many of the changes noted spatially and temporally in the IRL constitute disturbances to the system. The IRL, like many estuaries, experiences disturbances in the form of excess freshwater runoff (Salewski & Proffitt 2016) and tropical storm systems. Some of the effects are ephemeral and some cause unexpected consequences, such as shifts in dominance. Other effects can be longer lasting. The central IRL, for example, was impacted by 4 tropical weather systems between mid-August and late September 2004 (Steward et al. 2006). In the intertidal mangrove forests, storms caused considerable damage, and long-term recovery was delayed by the indirect or added effects of elevated nutrients (Feller et al. 2015). Conversely, in subtidal settings, high freshwater discharges dropped salinities by half, sediment was deposited, and turbidity and color increased by factors of nearly 3× and 10×, respectively. Some of these factors had not fully recovered to pre-storm levels by the next spring because of longer water residence times and a wetter than usual period of rainfall (Steward et al. 2006). However, only 1 of 25 seagrass sites was adversely affected by storm-related sedimentation, although in some areas there was a temporary shift in the dominant seagrass species that was attributed to low salinities (Steward et al. 2006). Longer-term through July 2006 there was an increase in bottom cover seagrass with depth, but a decrease in seagrass densities.

Although storms have acute effects that may not be long-lasting, the effects of disturbance in terms of light attenuation affecting seagrass has been occurring for decades. From the 1940s through 1992, the maximum depth at which seagrass occurred throughout the IRL decreased from 1.3–1.6 m to 0.8 m, with the greatest changes in the northern reaches (Fletcher & Fletcher 1995), which suggests long-term trends in decreasing water clarity. In more recent years, bloom conditions were found to affect light penetration and DO, which could impact other organisms, such as seagrasses and their denizens. Between 2009 and 2011 samplings, the IRL north of Sebastian Inlet experienced a seagrass decline from 70 238 to 38 322 acres (~28 424 to 15 508 ha), with a subsequent recovery by 2013 to 43 084 acres (17 435 ha; Morris et al. 2015). Die-off was patchy, with little or no loss in Mosquito Lagoon or the extreme northern end of the IRL proper north of Titusville. In the IRL proper north of Sebastian Inlet (i.e. corresponding to Regions 4 and 5 herein), there was 63.3 ± 36.8% (SD) loss, while south of Sebastian Inlet to around Vero Beach, losses totaled 56.2 ± 28.5%, and in the Banana River the seagrass loss was 87.4 ± 5.0% as calculated from data presented in Morris et al. (2015). This die-off co-occurred with 2 dense phytoplankton blooms (Phlips et al. 2015); the first, beginning in Fall 2010, was primarily cyanobacteria (chl a), diatoms (chl a and c), and dinoflagellates (chl a and c). The second larger bloom, the so-called 'superbloom,' started in Spring 2011 (SJRWMD 2012) and was dominated by small cyanobacteria and a chlorophyte putatively assigned to the class Pedinophyceae containing chl a and b (Phlips et al. 2015). These dense blooms reduced light penetration, which has been implicated as one of the causative agents of the seagrass die-off. After these blooms, a brown tide event occurred in the Mosquito Lagoon in

2012 (Gobler et al. 2013, Phlips et al. 2015) dominated by the pelagophyte *Aureoumbra lagunensis* (chl a and c), a species which previously had not bloomed in the IRL. The effects of this last bloom on seagrasses are not clear.

The SEM analyses conducted here lend support to many of the points regarding phytoplankton effects on seagrass. In the next section, the spatial and temporal differences that underlie some of the changes that produce elevated phytoplankton biomass in the IRL are highlighted. Also, the influences of phytoplankton biomass on several important ecological functions such as light penetration and nutrient regeneration are included in the SEM analyses of long-term data.

Analyzing spatial and temporal aspects of ecological topology using SEM

Cloern (2001) noted the importance of multiple stressors acting in concert and interactions among stressors and biota. Mallin et al. (1999) noted that a number of variables affected phytoplankton production in the Cape Fear River estuary. Here, both the entire IRL and regional partitioned SEM analyses indicate that phytoplankton biomass in the IRL is controlled by both direct and indirect effects of a suite of environmental drivers such as nutrients, temperature, light penetration, and salinity. Moreover, several ecological functions relating to light penetration and DO varied substantially with changes in biotic variables as well as physico-chemical drivers. This is consistent with Nielsen et al. (2002), who used path analysis to show that phytoplankton biomass had a direct effect on light penetration as well as an indirect effect through its contribution to total suspended matter. Despite these extreme differences in space and time, SEM analyses (the 'one SEM to rule them all' hypothesis) indicated that 46% of the variation in chl *a* can be explained by a complex network of linkages and interactions among biotic and environmental variables that in part accounts for the complex ecological topology in the IRL. The spatial variation is defined by differences in proximity to inlets, freshwater inputs, width of this long, narrow estuary, depth, sediment type, and position along a subtropical to temperate latitudinal gradient. The temporal differences are probably due to changes in urbanization (population size, numbers of septic tanks, etc.) and agricultural chemicals over the 2 decades of the study. Analyses also showed that biological–environmental feedback loops are important in the system and that selected ecological functions such as light penetration and DO content are in part due to biotic changes.

Temporal partitioning into 3 yr groups allowed evaluation of changes in drivers that were associated with the superbloom and other large blooms in longer residence time areas. A strong drought co-occurred with the large blooms of 2010–2012 which has prompted the suggestion that perhaps internal nutrient regeneration was a source of nutrients rather than runoff, which would have been rainfall dependent (SJRWMD 2012). The SEM tested herein can be used to determine if there is support for this idea in the monitoring data. In Fig. 9, part of the SEM and back-transformed (geometric) means for the 2010–2012 bloom period are compared with long-term geometric means of data collected prior to 2010. Prior to 2010, both TKN and TP increased with rainfall, and salinity decreased with rainfall although the effect sizes were small, possibly because of the month-long period between samplings (Fig. 9). However, during the bloom period, there was no significant effect of rainfall. For the 2010–2012 bloom period, the back transformed chl *a* mean of all water quality stations in Regions 4 to 7 was 11.41 µg l^{-1}, about 2× the long-term mean of 5.77 µg l^{-1} for these regions in previous times. Concentration of TP was greater during the bloom period, but TKN was not (Fig. 9). This led to TKN limitation and thus TKN being the dominant driver of chl *a* blooms, whereas prior to 2010, the long-term average dominant driver was TP (Fig. 9). However, both TKN and TP had important effects on chl *a* during the bloom period and before. These results are also consistent with Lapointe et al. (2015), who reported that nitrogen-laden sewage runoff following the breaking of drought conditions is in part responsible for phytoplankton and macroalgal blooms.

Within-region nutrient regeneration can be assessed by comparing the decomposition pathway from phaeophytin to nutrients for bloom and pre-bloom periods. The path Phaeo→TKN was essentially the same in pre-bloom and bloom periods, but the path Phaeo→TP more than doubled in effect size during the bloom period (Fig. 9). Thus, TP was being regenerated at a much greater rate during the blooms, which may account for the high concentrations of TP during this time. This regeneration was part of the feedback loop involving nutrients, chl *a*, and its breakdown product, phaeophytin. It is unclear why TKN did not show the same regeneration. Perhaps spatial variability or denitrification or other processes not included in the SEM affected nitrogen.

Also, self-limitation of phytoplankton biomass by means of a reduction of light penetration in the pre-

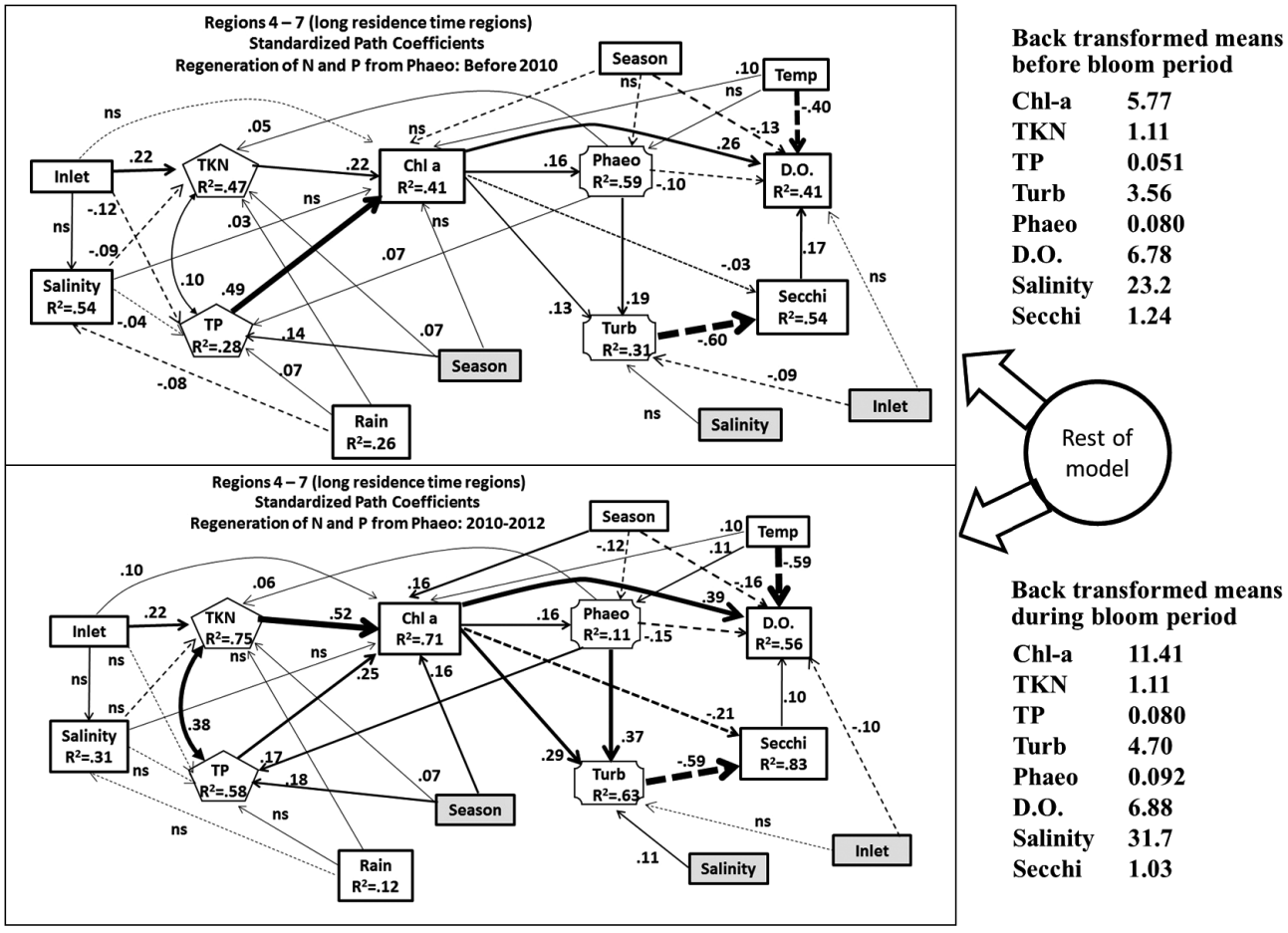

Fig. 9. Part of the structural equation model (SEM) for Regions 4 to 7 before 2010 (top) and from 2010–2012 (bottom). Back-transformed geometric means of variables are also presented for these periods. Note paths from Phaeo to TKN and TP that constitute part of the feedback loop of Nutrients→Chl *a*→Phaeo→Nutrients. The strength of the path (standardized path coefficient) from Phaeo→TKN was essentially unchanged before and during the blooms as was the resulting concentration of TKN, but that of the path from Phaeo→TP nearly doubled as did the concentration of TP. The excess of TP resulted in limitation by TKN, and thus nitrogen became the dominant driver of the phytoplankton blooms

vious month was small prior to 2010 in Regions 4 to 7 in terms of the long-term average path coefficient (L1Turb→Chl*a* = –0.04), but was 3× this size during the bloom period (path coefficient L1Turb→Chl*a* = –0.12). In Regions 4 to 7, mean Secchi disk depth was reduced 17% from 1.24 m prior to 2010 to 1.03 m during the 2010–2012 bloom period. The mean reduction in light penetration may not be sufficient to limit algal growth, but of course, in some months and seasons the light penetration was substantially less during the bloom period and may have been limiting to both phytoplankton and seagrass. This is consistent with Nielsen et al. (2002), who used path analysis to show that phytoplankton biomass had a direct effect on light penetration as well as an indirect effect through its contribution to total suspended matter.

Exploring relative dominance by comparing the responses of chl *b* and *c* to that of chl *a* is not the optimal method because different taxonomic groups are included in the chl *c* measure. However, these were the data available in the monitoring dataset and provide some insight into responses by different taxonomic groups. Obayashi et al. (2001) used various pigments to assess phytoplankton community structure, although they used pigments not available here for finer-scale separation of taxa. Total phytoplankton biomass (chl *a*) was correlated with chl *c*, suggesting that the most common taxa, in most places in the IRL, at most times were dinoflagellates, diatoms, and others. Chl *b* concentrations were low and were more weakly correlated with chl *a*, indicating that chlorophytes and euglenoids were less common components of the phytoplankton at most times in

most locations. Although there was a small direct effect of summer season on chl *a*, the total effects when all indirect pathways were included was 0.16, which is in the moderate effect size range. Total effects of season on chl *c* (standardized coefficient = 0.07) was much smaller despite the high correlation between chl *a* and *c*. The small negative total effect of season on chl *b* (–0.10) indicates that these taxa are in greater abundance in the dry winter season. In the IRL, considerable variation in chl *a*, *b*, and *c* occurred because of the differences in both spatial and temporal components of the ecosystem.

Synthesis

SEM facilitates assigning causality to such assessments by casting the complex web of interactions as a single multivariate hypothesis and testing this for fit to the data. Classically trained experimental ecologists may object to calling this cause-and-effect analysis because the data are observationally rather than experimentally derived. However, in terms of answering questions of ecological importance, it matters little if it is termed 'causal' or 'presumptively causal pending confirmation by future studies.' For large problems of real-world complexity, this approach is clearly better than piecing together the results of multiple experiments that usually occur over short time periods and small spatial scales. While providing valuable insight into direct effects of certain variables over some spatial and temporal scales, experiments cannot begin to address the complex web of direct and indirect effects inherent in ecological systems. Sometimes not taking the covariance between 2 (or more) variables into account can even lead to spurious results (see Harnik 2011). Nor do the results from small-scale studies often scale up to the real world of multifaceted ecosystems and landscapes where response variables are influenced by many factors not included in the experiment. SEM also assists in untangling the suites of indirect effects along paths between variables and understanding the total effects (sum of direct and indirect paths) of predictors on responses.

The following approach can be a model for analyses of ecological problems in estuaries. First, establish a conceptual model containing both proposed cause-and-effect and strictly correlative pathways that constitutes a multivariate hypothesis. Second, convert this to a structural equation model and use it to analyze monitoring data gathered independently, meaning do not pre-analyze the data in order to develop the pathways! Third, confirm the hypothesis (or falsify its null version) if the covariance structure of the SEM fits the covariance structure in the monitoring data. Using a panel model approach with time lags or, where the data permit, a longitudinal growth curve model, both temporal and spatial variation can be included in the analyses.

Acknowledgements. I thank the SFWMD and SJRWMD for the foresight to engage in long-term monitoring in the IRL, because those data provide a strong scaffold of support for research on a wide variety of estuarine ecology questions. Special thanks to Wendy Tweedale for compiling the SJRWMD data and to her and Margaret Lasi for answering questions about their data. Another special thank you to Laura Herren (previously at Harbor Branch), who provided the map of the IRL. I also thank various staff members at SFWMD who answered questions about how to retrieve data from DBHYDRO. Nikki Dix, Paul Hargraves, Brian LaPointe, and Donna Devlin provided exceptionally useful feedback on earlier versions of my analyses, a cutoff for calling phytoplankton biomass a bloom or not (10 µg l^{-1}), the nature and direction of some causal pathways in the SEM, and the need for feedback loops in the final model, and were helpful by answering questions about phytoplankton and water quality. Donna Devlin, Margaret Lasi, and the 2016 FAU Scientific Communication class (especially H. Standish, S. Grolesh, C. Peccione, J. Cutter, S. Huff, and J. Byrum) provided very helpful comments at various stages of analysis and writing of the manuscript. Jim Grace and Jarrett Byrnes kindly answered my questions about structural equation modeling of time-series data.

LITERATURE CITED

Anderson DM, Glibert PM, Burkholder JM (2002) Harmful algal blooms and eutrophication: nutrient sources, composition, and consequences. Estuaries 25:704–726

Arhonditsis GB, Stow GA, Paerl HW, Valdes-Weaver LM, Steinberg LJ, Reckhow KH (2007) Delineation of the role of nutrient dynamics and hydrologic forcing on phytoplankton patterns along a freshwater-marine continuum. Ecol Model 208:230–246

Cloern JE (2001) Our evolving conceptual model of the coastal eutrophication problem. Mar Ecol Prog Ser 210: 223–253

Danger M, Daufresne T, Lucas F, Pissard S, Lacroix G (2008) Does Liebig's Law of the Minimum scale up from species to communities? Oikos 117:1741–1751

Dawes C, Hanisak MD, Kenworthy WJ (1995) Seagrass biodiversity in the Indian River Lagoon. Bull Mar Sci 57: 59–66

Feller IC, Dangremond EM, Devlin DJ, Lovelock CE, Proffitt CE, Rodriguez W (2015) Nutrient enrichment intensifies hurricane damage and prolongs recovery in mangrove ecosystems in the Indian River Lagoon. Ecology 96: 2960–2972

Fletcher SW, Fletcher WW (1995) Factors affecting changes in seagrass distribution and diversity patterns in the Indian River Lagoon Complex between 1940 and 1992. Bull Mar Sci 57:49–58

Glibert PM, Wazniak CE, Hall MR, Sturgis B (2007) Seasonal and interannual trends in nitrogen and brown tide in Maryland's coastal bays. Ecol Appl 17(Suppl):S79–S87

Gobler CJ, Koch F, Kang Y, Berry DL and others (2013) Expansion of harmful brown tides caused by the pelagophyte *Aureoumbra lagunensis* DeYoe et Stockwell, to the US East coast. Harmful Algae 27:29–41

Grace JB (2006) Structural equation modeling in natural systems. Cambridge University Press, New York, NY

Grace JB, Anderson M, Olff H, Scheiner S (2010) On the specification of structural equation models for ecological systems. Ecol Monogr 80:67–87

Harnik PG (2011) Direct and indirect effects of biological factors on extinction risk in fossil bivalves. Proc Natl Acad Sci USA 108:13594–13599

Harpole WS, Ngai JT, Cleland EE, Seabloom EW and others (2011) Nutrient co-limitation of primary producer communities. Ecol Lett 14:852–862

Kemp WM, Boynton WR, Adolf JE, Boesch DF and others (2005) Eutrophication of Chesapeake Bay: historical trends and ecological interactions. Mar Ecol Prog Ser 303:1–29

Lapointe BE, Herren LW, Debortoli DD, Vogel MA (2015) Evidence of sewage-driven eutrophication and harmful algal blooms in Florida's Indian River Lagoon. Harmful Algae 43:82–102

Mallin MA, Cahoon LB, McIver MR, Parsons DC, Shank GC (1999) Alternation of factors limiting phytoplankton production in the Cape Fear River estuary. Estuaries 22: 825–836

Malone TC, Conley DJ, Fisher TR, Gilbert PM, Harding LW, Sellner KG (1996) Scales of nutrient-limited phytoplankton productivity in Chesapeake Bay. Estuaries 19:371–385

Morris L, Chamberlain R, Jacoby C (2015) Summary report for the Northern Indian River Lagoon. In: Yarbro LA, Carlson PR (eds) Seagrass Integrated Mapping and Monitoring Program mapping and monitoring report no. 1.1. Tech Rep TR-17. Florida Fish and Wildlife Research Institute, St Petersburg, FL

Muthén LK, Muthén BO (2010) Mplus users guide, 6th edn. Muthén & Muthén, Los Angeles, CA

Nielsen SL, Sand-Jensen K, Borum J, Geertz-Hansen O (2002) Phytoplankton, nutrients, and transparency in Danish coastal waters. Estuaries 25:930–937

Obayashi Y, Tanoue E, Suzuki K, Handa N, Nojiri Y, Wong CS (2001) Spatial and temporal variabilities of phytoplankton community structure in the northern North Pacific as determined by phytoplankton pigments. Deep Sea Res I 48:439–469

Pennock JR, Sharp JH (1994) Temporal alternation between light- and nutrient-limitation of phytoplankton production in a coastal plain estuary. Mar Ecol Prog Ser 111: 275–288

Phlips EJ, Badylak S, Christman M, Wolny J and others (2011) Scales of temporal and spatial variability in the distribution of harmful algae species in the Indian River Lagoon, Florida, USA. Harmful Algae 10:277–290

Phlips EJ, Badylak S, Lasi MA, Chamberlain R and others (2015) From red tides to green and brown tides: bloom dynamics in a restricted subtropical lagoon under shifting climatic conditions. Estuaries Coasts 38:886–904

Salewski E, Proffitt CE (2016) Separate and combined effects of estuarine stress gradients and disturbance on oyster population development on restored reefs. Estuaries Coasts 39:510–528

Shipley B (2000) Cause and correlation in biology. Cambridge University Press, New York, NY

Short FT, Montgomery J, Zimmerman CF, Short CA (1993) Production and nutrient dynamics of a *Syringodium filiforme* Kütz. seagrass bed in Indian River Lagoon, Florida. Estuaries 16:323–334

Sigua GC, Steward JS, Tweedale WA (2000) Water quality monitoring and biological integrity assessment in the Indian River Lagoon, Florida: status, trends, and loadings (1988–1994). Environ Manag 25:199–209

Silvertown J, Poulton P, Johnston E, Edwards G, Heard M, Biss PM (2006) The Park Grass Experiment 1856–2006: its contribution to ecology. J Ecol 94:801–814

SJRWMD (St. Johns River Water Management District) (2012) Indian River Lagoon 2011 Superbloom Plan of Action. Tech Rep. http://www.sjrwmd.com/indianriverlagoon/technicaldocumentation/pdfs/2011superbloom_investigationplan_June_2012.pdf

Smith NP (1993) Tidal and nontidal flushing of Florida's Indian River Lagoon. Estuaries 16:739–746

Smith V (2006) Responses of estuarine and coastal marine phytoplankton to nitrogen and phosphorus enrichment. Limnol Oceanogr 51:377–384

Steward JS, Virnstein RW, Lasi MA, Morris LJ, Miller JD, Hall LM, Tweedale WA (2006) The impacts of the 2004 hurricanes on hydrology, water quality, and seagrass in the Central Indian River Lagoon, Florida. Estuaries Coasts 29:954–965

Thompson MJ (1978) Species composition and distribution of seagrass beds in the Indian River Lagoon. Fla Sci 41:90–96

Thompson JN, Reichman OJ, Morin PJ, Polis GA and others (2001) Frontiers of ecology. Bioscience 51:15–24

Whitehouse LNA, LaPointe B (2015) Comparative ecophysiology of bloom-forming macroalgae in the Indian River Lagoon, Florida: *Ulva lactuca, Hypnea musciformis*, and *Gracilaria tikvahiae.* J Exp Mar Biol Ecol 471:208–216

Yin K (2002) Monsoonal influence on seasonal variations in nutrients and phytoplankton biomass in coastal waters of Hong Kong in the vicinity of the Pearl River estuary. Mar Ecol Prog Ser 245:111–122

Yin K, Qian PY, Chen JC, Hsieh DPH, Harrison PJ (2000) Dynamics of nutrients and phytoplankton biomass in the Pearl River estuary and adjacent waters of Hong Kong during summer: preliminary evidence for phosphorus and silicon limitation. Mar Ecol Prog Ser 194:295–305

Editorial responsibility: Katherine Richardson, Copenhagen, Denmark

Submitted: February 1, 2016; Accepted: February 9, 2017
Proofs received from author(s): March 30, 2017